

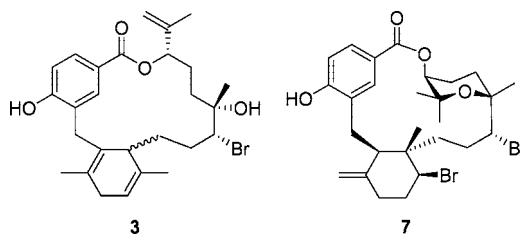
Antimalarial Bromophycolides J–Q from the Fijian Red Alga
Callophycus serratus

Amy L. Lane,^{†,‡} E. Paige Stout,^{†,‡} An-Shen Lin,[§] Jacques Prudhomme,^{||} Karine Le Roch,^{||}
Craig R. Fairchild,[⊥] Scott G. Franzblau,[#] Mark E. Hay,[§] William Aalbersberg,[∇] and
Julia Kubanek^{*,†,§}

School of Chemistry and Biochemistry and School of Biology, Georgia Institute of Technology, Atlanta, Georgia 30332, Department of Cell Biology and Neuroscience, University of California—Riverside, Riverside, California 92521, Bristol-Myers Squibb Pharmaceutical Research Institute, Princeton, New Jersey 08543, Institute for Tuberculosis Research, College of Pharmacy, University of Illinois at Chicago, Chicago, Illinois 60612, and Institute of Applied Sciences, University of the South Pacific, Suva, Fiji

julia.kubanek@biology.gatech.edu

Received January 2, 2009



Bromophycolides J–Q (1–8) were isolated from extracts of the Fijian red alga *Callophycus serratus* and identified with 1D and 2D NMR spectroscopy and mass spectral analyses. These diterpene–benzoate macrolides represent two novel carbon skeletons and add to the 10 previously reported bromophycolides (9–18) from this alga. Among these 18 bromophycolides, several exhibited activities in the low micromolar range against the human malaria parasite *Plasmodium falciparum*.

Introduction

Over 500 million cases of malaria are reported annually, causing 1–3 million deaths worldwide.¹ Although several antimalarial drugs are currently on the market, resistance to these treatments is on the rise, thus providing an increasing need for novel antimalarial medicines.² As a recognized source of pharmacologically active natural products,^{3,4} marine organisms such as macroalgae may offer unique natural products for the development of novel treatments for malaria and other infectious diseases.

From the Fijian red alga *Callophycus serratus*, we previously reported the discovery of 10 bromophycolides, unusual C₂₇ diterpene–benzoate macrolides.^{5,6} Exploration of additional *C. serratus* collections then led to discovery of 10 novel callophycoic acids and callophycols, C₂₇ diterpene–benzoic acids, and C₂₆ diterpene–phenols.⁷ Herein, we report identification of eight additional macrolides, bromophycolides J–Q (1–8), representing two novel carbon skeletons, two isomeric macrolides possessing a tetrahydropyran ring, two regioisomers of the known bromophycolide E (13), and a regioisomer of bromophycolide A (9) and adding further evidence that this red alga is an abundant source of chemically diverse and biologically active natural products.

[†] School of Chemistry and Biochemistry, Georgia Institute of Technology.

[‡] These authors contributed equally to this work.

[§] School of Biology, Georgia Institute of Technology.

^{||} Department of Cell Biology and Neuroscience, University of California Riverside.

[⊥] Bristol-Myers Squibb Pharmaceutical Research Institute.

[#] Institute for Tuberculosis Research, University of Illinois at Chicago.

[∇] Institute of Applied Sciences, University of the South Pacific.

(1) Snow, R. W.; Guerra, C. A.; Noor, A. M.; Myint, H. Y.; Hay, S. I. *Nature* **2005**, *434*, 214–217.

(2) Hyde, J. E. *FEBS J.* **2007**, *274*, 4688–4698.

(3) Faulkner, D. J. *Nat. Prod. Rep.* **2000**, *17*, 1–6.

(4) Blunt, J. W.; Copp, B. R.; Hu, W. P.; Munro, M. H. G.; Northcote, P. T.; Prinsep, M. R. *Nat. Prod. Rep.* **2008**, *25*, 35–94.

(5) Kubanek, J.; Prusak, A. C.; Snell, T. W.; Giese, R. A.; Fairchild, C. R.; Aalbersberg, W.; Hay, M. E. *J. Nat. Prod.* **2006**, *69*, 731–735.

(6) Kubanek, J.; Prusak, A. C.; Snell, T. W.; Giese, R. A.; Hardcastle, K. I.; Fairchild, C. R.; Aalbersberg, W.; Raventos-Suarez, C.; Hay, M. E. *Org. Lett.* **2005**, *7*, 5261–5264.

(7) Lane, A. L.; Stout, E. P.; Hay, M. E.; Prusak, A. C.; Hardcastle, K.; Fairchild, C. R.; Franzblau, S. G.; Le Roch, K.; Prudhomme, J.; Aalbersberg, W.; Kubanek, J. *J. Org. Chem.* **2007**, *72*, 7343–7351.

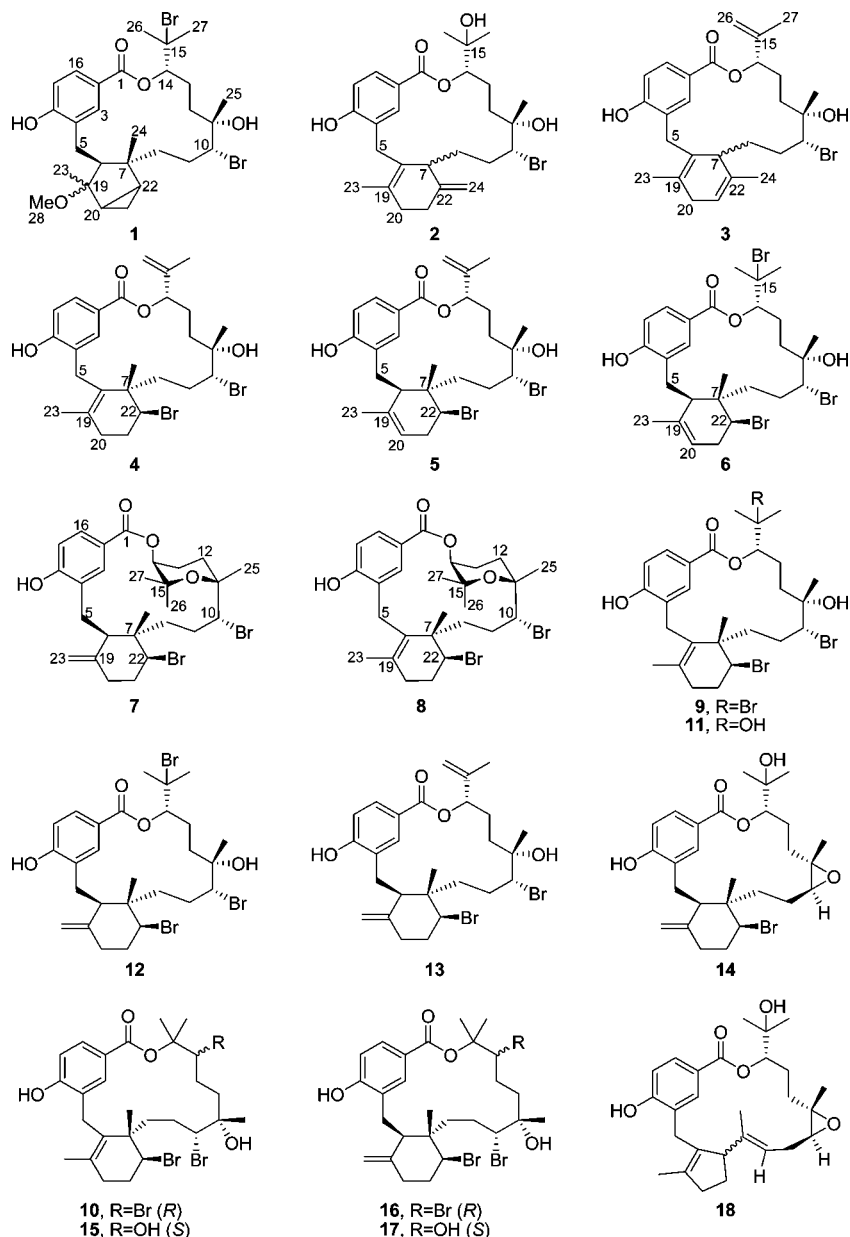


FIGURE 1. Novel bromophycolides J–Q (**1–8**) and previously reported bromophycolides A–I (**9–17**) and debromophycolide A (**18**) from *Callophycus serratus*.

Results and Discussion

Following the isolation and identification of 10 bromophycolides from *C. serratus*,^{5,6} LC–MS evaluation of extracts from a Yanuca (Fiji) collection of this red macroalga suggested the presence of additional bromophycolide-like metabolites. Reversed- and normal-phase HPLC yielded eight novel metabolites, bromophycolides J–Q (**1–8**, Figure 1), in quantities sufficient for structure elucidation.

A molecular formula of $C_{28}H_{40}O_5Br_2$ was established for bromophycolide J (**1**), based on a mass spectral parent ion at m/z 613.1160, supported by a dibrominated isotopic splitting pattern. Inspection of 1H , ^{13}C , HSQC, HMBC, and COSY NMR spectral data for **1** revealed a 4-hydroxybenzoyl group common to all bromophycolides (Table 1, Supporting Information).^{5,6} Comparison of spectral data for **1** with bromophycolide A (**9**)

supported a bromine-substituted isopropyl group at the diterpene head and established diterpene–aryl connectivity identical to that of **9**.⁶

Further comparison of NMR spectral data for **1** and **9** revealed substantial differences between these two natural products only in the vicinity of the carbocyclic terpene ring.⁶ For **1**, HMBC correlations from Me-23 (δ 1.38) to C-6 (δ 45.5), C-19 (δ 89.8), and C-20 (δ 28.0) established C-6–C-19–C-20 connectivity. An HMBC correlation from OMe-28 (δ 3.33) to C-19 established quaternary C-19 as the site of attachment for OMe-28 and Me-23. HMBC correlations from Me-24 (δ 0.55) to C-6, C-7 (δ 45.8), and C-22 (δ 31.9) established connectivity between these carbons. COSY correlations between H-22 (δ 1.14) and both H-21 protons (δ 0.31, 0.42), between H-20 (δ 1.55) and both H-21 protons, and between H-22 and H-20, as well as the shielded chemical shift observed for methylene C-21 (^{13}C δ 8.5)

TABLE 1. ^{13}C and ^1H NMR Spectral Data for Bromophycolides J–Q (1–8) (500 MHz; in CDCl_3)^a

	1		2		3		4		5		6		7		8		
	$\delta^{13}\text{C}$	$\delta^1\text{H}$ (J_{HH})	$\delta^{13}\text{C}$	$\delta^1\text{H}$ (J_{HH})	$\delta^{13}\text{C}$	$\delta^1\text{H}$ (J_{HH})	$\delta^{13}\text{C}$	$\delta^1\text{H}$ (J_{HH})	$\delta^{13}\text{C}$	$\delta^1\text{H}$ (J_{HH})	$\delta^{13}\text{C}$	$\delta^1\text{H}$ (J_{HH})	$\delta^{13}\text{C}$	$\delta^1\text{H}$ (J_{HH})	$\delta^{13}\text{C}$	$\delta^1\text{H}$ (J_{HH})	
1	165.6	167.6	165.9	165.3	164.7	163.0	164.7	165.5	164.9	165.0	164.9	165.5	164.9	165.0	165.0		
2	121.2	122.8	122.9	122.5	123.0	122.5	123.0	123.0	123.0	123.0	123.0	123.0	123.1	122.9	122.9		
3	130.1	8.11 brs	133.3	7.67 d (1.7)	131.4	7.82 s	130.6	7.85 brs	129.5	7.82 s	130.6	7.85 brs	131.4	8.06 d (1.6)	129.8	7.64 s	
4	128.3	125.4	124.6	126.4	129.5	126.4	126.4	126.4	129.5	126.4	128.4	128.4	128.7	128.2	128.2		
5	27.1	2.37 d (15)	29.4	3.29 d (15)	29.7	3.22 d (15)	28.5	3.24 d (8.8)	27.3	2.60 d (15)	25.8	2.82 m, 2.98 d (13)	25.5	2.61 d (15)	28.3	3.15 d (17)	3.65 d (17)
6	45.5	2.59 m	138.6	3.64 d (15)	132.6	3.46 d (15)	130.8	3.57 d (18)	47.8	2.83 dd (15, 9.0)	43.7	2.84 m	51.1	3.17 dd (15, 8.0)	131.0		
7	45.8	50.6	49.0	43.4	41.3	41.3	43.4	40.9	47.8	2.67 m	40.9	44.7	44.7	43.9	43.9		
8	42.7	1.21 m	30.0	1.45 m	37.2	1.58 m	37.6	1.58 m	37.2	1.58 m	36.6	1.23 m, 2.08 m	37.4	1.71 m, 2.13 m	37.7	1.58 m, 1.80 m	
9	31.3	1.37 m	31.9	1.44 m	30.7	2.44 m	28.8	1.93 m	26.0	2.20 m, 2.39 m	28.5	1.98 m, 2.00 m	25.2	2.14 m, 2.58 m	27.2	2.05 m, 2.28 m	
10	70.5	3.99 d (11)	72.0	3.96 m	67.8	3.97 dd (11, 3)	71.5	3.82 d (8.8)	70.0	4.20 d (11)	70.0	3.79 d (11)	64.7	4.43 dd (11, 2.5)	63.1	4.46 dd (12, 2.5)	
11	72.5	73.3	73.0	73.4	74.4	73.4	73.4	73.4	74.4	74.4	73.0	73.0	76.0	76.1	76.1		
12	35.4	1.50 m	32.6	1.24 m	31.6	1.67 m	33.3	1.52 m	32.2	1.86 m	33.8	1.53 m, 1.98 m	26.5	1.72 m, 2.35 m	25.8	1.69 m, 2.20 m	
13	26.4	2.11 m	23.6	1.83 m	25.8	1.73 m	28.6	1.79 m	27.0	1.70 m	26.4	2.13 m, 2.47 m	21.8	1.88 m, 2.30 m	21.9	1.80 m, 2.24 m	
14	80.5	4.88 d (11)	81.5	4.97 dd (2.7, 12)	74.9	5.52 brs	76.3	5.36 d (6.8)	76.0	5.23 brs	79.2	5.00 dd (9.4, 3.4)	70.6	5.08 dd (6.6, 1.7)	70.9	4.94 d (7.0)	
15	66.2	72.1	140.7	142.6	140.9	142.6	142.6	142.6	140.9	140.9	66.5	74.4	74.4	73.6	73.6		
16	129.6	7.81 d (8.0)	129.5	7.74 dd (1.8, 8.4)	129.2	7.75 dd (8.4, 1.9)	129.7	7.82 d (8.3)	129.3	7.75 d (7.9)	129.3	7.74 d (8.3)	128.6	7.70 dd (8.3, 1.9)	129.0	7.77 d (8.5)	
17	115.5	6.78 d (8.2)	115.9	6.81 d (8.4)	115.2	6.78 d (8.3)	115.2	6.80 d (8.3)	115.6	6.76 d (8.3)	115.7	6.81 d (8.3)	115.8	6.73 d (8.3)	115.0	6.80 d (8.5)	
18	157.8	159.1	158.0	157.5	156.6	157.5	157.5	157.5	156.6	156.6	156.5	156.5	156.9	157.1	157.1		
19	89.8	132.7	136.8	132.6	137.2	132.6	132.6	132.6	137.2	137.2	135.8	145.7	145.7	132.9	132.9		
20	28.0	1.55 m	36.7	2.24 m	37.8	2.30 m	32.4	2.13 m	120.3	5.19 m	119.4	5.33 brs	37.5	1.97 m, 2.34 m	32.6	2.05 m, 2.20 m	
21	8.5	0.31 m	36.0	1.95 m	122.5	4.81 t (6.5)	29.9	2.25 m	34.4	2.53 m	34.0	2.65 m	34.8	2.08 m, 2.22 m	30.7	2.20 m, 2.28 m	
22	31.9	1.14 m	150.3	-	138.8	-	61.3	4.49 dm (9.5)	59.8	4.28 dd (11, 5.3)	60.2	4.24 dd (6.8, 6.2)	62.0	4.33 dd (12, 4.1)	62.1	4.57 d (10)	
23	19.8	1.38 s	14.1	1.91 s	14.0	1.89 s	20.8	1.41 s	20.9	1.50 s	22.0	1.65 s	110.5	4.89 s, 5.30 s	20.7	1.34 s	
24	20.0	0.55 s	108.6	4.46 s	18.2	1.38 s	26.0	1.27 s	17.1	1.06 s	18.8	0.89 s	17.5	0.99 s	27.8	1.34 s	
25	29.0	1.17 s	26.1	1.26 s	27.5	1.30 s	30.2	1.26 s	28.0	1.40 s	29.3	1.32 s	27.0	1.47 s	27.5	1.42 s	
26	31.2	1.80 s	25.6	1.31 s	111.5	4.98 s	111.3	4.92 s	111.0	4.84 s	30.2	1.81 s	26.3	1.36 s	26.6	1.34 s	
27	30.5	1.78 s	26.8	1.31 s	19.5	1.79 s	19.2	1.80 s	19.7	1.79 s	31.5	1.83 s	27.8	1.09 s	27.6	1.15 s	
28	49.9	3.33 s															
OH	6.05 brs																
																	5.28 brs

^abr = broad; s = singlet; d = doublet; dd = doublet of doublets; t = triplet; m = multiplet.

prompted assignment of a cyclopropyl moiety comprised of C-20, C-21, and C-22. HMBC and COSY correlations established connection between this ring system and the benzoate system via C-5, analogous to previously identified metabolites.^{5,6}

Stereochemical assignments for **1** were facilitated by comparison of ¹H–¹H scalar couplings and NOE correlations with **9**.⁶ Observation of predicted scalar couplings and NOE correlations for **1** (Table 1, Supporting Information) prompted assignment of 10*R*,11*S*,14*S* stereochemistry as for **9**, whose absolute configuration was previously established by X-ray crystallography.⁶ Given a proposed, common biogenesis and an observed NOE between H-5b (δ 2.69) and Me-24, it seemed highly probable that a 7*R* configuration would also be shared between **1** and **9**. NOE correlations between H-6 (δ 2.59) and H-20, but not between H-6 and Me-24, established a 6*S* stereocenter. This assignment matched absolute configurations reported for all bromophycolides bearing a stereocenter at this site (e.g., bromophycolide D (**12**)).⁵ Due to difficulties assigning stereochemistry of 5-membered rings from NOE data, the configurations of C-19, C-20, and C-22 were not assigned at this time.

Bromophycolide K (**2**) was assigned a molecular formula of C₂₇H₃₇O₅Br from the parent ion observed at *m/z* 519.1767 ([M – H][–]). Comparison of ¹H, ¹³C, HSQC, HMBC, and COSY NMR spectral data with known bromophycolides confirmed a 15-membered macrolide framework analogous to **1** and **9** (Supporting Information).^{5,6} For **2**, a hydroxy substituent was assigned at C-15 (δ 72.1) on the basis of ¹³C NMR chemical shift precedents.^{5,6} As with **1**, HMBC and COSY correlations suggested that **2** diverged from other bromophycolides within the terpene carbocyclic moiety. Within this group, observation of HMBC correlations from Me-23 (δ 1.91) to C-6 (δ 138.6), C-19 (δ 132.7), and C-20 (δ 36.7) and from H-5a (δ 3.29) to C-7 (δ 50.6) established the tetrasubstituted olefin. COSY correlations from both H-20 protons (δ 2.24, 2.37) to both H-21 protons (δ 1.95, 2.17) and HMBC correlations from both H-24 protons (δ 4.46, 4.66) to C-7 and C-21 (δ 36.0) closed the six-membered ring containing exo- and endocyclic double bonds.

High-resolution mass spectral data indicated that bromophycolide L (**3**) differed from **2** by a loss of one H₂O molecule, displaying an [M – H][–] *m/z* of 501.1677, appropriate for a molecular formula of C₂₇H₃₅O₄Br. HMBC correlations from Me-27 (δ 1.79) to C-14 (δ 74.9), C-15 (δ 140.7), and C-26 (δ 111.5) suggested an isopropenyl diene head identical with that of bromophycolide E (**13**) (Table 1).⁵ Likewise, HMBC correlations from both H-26 vinyl protons (δ 4.98, 5.07) to C-14, C-15, and C-27 (δ 19.5) confirmed this connectivity. Evaluation of ¹H, COSY, and HMBC NMR spectral data of **3** to that of **2** indicated an additional difference within the terpene carbocyclic system. HMBC correlations from Me-24 (δ 1.38) to C-7 (δ 49.0), C-21 (δ 122.5), and C-22 (δ 138.8) suggested that the rearranged terpene skeleton was present as in **2**; however, the unsaturation was determined to be endocyclic at Δ^{21,22} through COSY correlations of olefinic H-21 (δ 4.81) with H-20b (δ 2.42) and a weak long-range COSY correlation between H-21 and Me-24 (Supporting Information).

For **3**, similar NOEs were observed as for bromophycolide E (**13**), suggesting a 10*R*,11*S*,14*S* configuration (Supporting Information).⁵ NOEs were present between H-7 (δ 3.41) and H-20b, located 1,4 relative to each other across their six-membered ring, thus suggesting a pseudoboat conformation of this ring. The lack of stereocenters near C-7 prevented stereo-

chemical assignment at this position in either **2** or **3**, given that an *R* or *S* configuration would be expected to result in NOEs between the axial protons H-7 and H-20b.

Bromophycolide M (**4**) exhibited a molecular formula of C₂₇H₃₆O₄Br₂ ([M – H][–] *m/z* 581.0906), isomeric to **13**.⁵ A combination of 1D and 2D NMR spectral data for **4** supported assignment of a carbon skeleton and most functionalities identical to that of **13**. For **4**, HMBC correlations from Me-23 (δ 1.41) to fully substituted olefinic carbons C-6 (δ 130.8) and C-19 (δ 132.6) as well as to C-20 (δ 32.4) suggested regioisomerization of the carbon–carbon double bond relative to **13**. Finally, 7*S*,10*R*,11*S*,14*S*,22*S* stereochemistry was proposed for **4**, based on comparison of NOE correlations with those of **9** and **13** (Supporting Information).

The mass spectrum of bromophycolide N (**5**), with [M – H][–] *m/z* of 581.0907, suggested yet another regioisomer of **13**, with a molecular formula of C₂₇H₃₆O₄Br₂. Comparison of ¹H, COSY, and HMBC NMR spectral data of **5** with that of **4** and **13** suggested a difference in the cyclohexenyl double bond. HMBC correlations observed from Me-23 (δ 1.50) to C-6 (δ 47.8), C-19 (δ 137.2), and C-20 (δ 120.3), along with COSY correlations between both H-5 protons (δ 2.60, 2.83) and H-6 (δ 2.67), supported the Δ^{19,20} assignment. Because similar NOEs were observed for **5** as for **4** and **13**, 6*R*,7*S*,10*R*,11*S*,14*S*,22*S* stereochemistry was proposed for **5** (Supporting Information).

Bromophycolide O (**6**) exhibited an [M – H][–] *m/z* of 661.0182 with a tribrominated isotopic pattern, appropriate for a molecular formula of C₂₇H₃₇O₄Br₃ as seen with bromophycolides A (**9**), B (**10**), and D (**12**). Inspection of 1D and 2D NMR spectral data of **6** suggested yet another 15-membered macrocyclic skeleton. As with **5**, regioisomerization of the cyclohexenyl double bond to Δ^{19,20} was supported by observation of HMBC correlations from Me-23 (δ 1.65) to C-6 (δ 43.7), C-19 (δ 135.8), and C-20 (δ 119.4), as well as COSY correlations between H-5a (δ 2.82) and H-6 (δ 2.84) and a long-range COSY correlation between Me-23 and H-20 (δ 5.33). Similar NOEs were observed for **6** as with **9** and **12**; thus, a 6*R*,7*S*,10*R*,11*S*,14*S*,22*S* stereochemistry was inferred for **6** (Supporting Information).

Bromophycolide P (**7**) also displayed the same mass spectral parent ion as **4**, **5**, and **13**, with an [M – H][–] *m/z* ion of 581.0865, appropriate for a molecular formula of C₂₇H₃₆O₄Br₂. Comparison of spectral data of **7** with other known bromophycolides supported another 15-membered macrocycle. HMBC correlations from both H-23 protons (δ 4.89, 5.30) to C-6 (δ 51.5) and C-20 (δ 37.5), as well as correlations from both H-5 protons (δ 2.61, 3.17) to C-6 and C-19 (δ 145.7), indicated the presence of an exomethylene group (C-23, δ 110.5). Interestingly, carbon chemical shifts of **7** significantly differed from other known *C. serratus* natural products at C-12 (δ 26.5) and C-13 (δ 21.8). Having assigned all olefinic carbons and protons, one ring remained unaccounted for in **7** based on the index of hydrogen deficiency; thus, a third six-membered ring was assigned via an ether linkage between C-11 (δ 76.0) and C-15 (δ 74.4), which accounted for the differences seen in the carbon chemical shifts at C-12 and C-13. Moreover, the phenolic hydroxyl proton (δ 5.68) was observed in the ¹H NMR spectrum, providing evidence that the ether linkage did not involve this position (C-18, δ 156.9). However, another possibility was that rather than an ether linkage, both C-11 and C-15 were hydroxylated, and the ESI-MS ion observed at *m/z* 581.0865 resulted from dehydration at C-11 or C-15 during ionization.

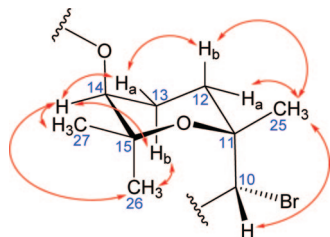


FIGURE 2. Key NOE correlations (double-headed arrows) observed for bromophycolide P (**7**) established the stereochemistry around the tetrahydropyran ring as 10*R*,11*R*,14*S*.

In order to test this hypothesis, **7** was acetylated and then subjected to ^1H NMR spectroscopy (data not shown). Only one acetyl group was observed in the ^1H NMR spectrum, rejecting the notion of a polyhydroxylated natural product and confirming the presence of a single free, phenolic hydroxyl group along with the tetrahydropyran ring in **7**.

Retention of the 6*R*,7*S*,10*R*,22*S* configuration of **7** was proposed by comparison of NOEs for **7** with other bromophycolides possessing the C-19–C-23 unsaturation (e.g., **12**–**14**, **16**–**17**, Figure 1, Supporting Information)⁵ and by inferring a common biosynthetic origin. NOEs observed between H-14 (δ 5.08) and both H-13s (δ 1.88, 2.30), Me-26 (δ 1.36), and Me-27 (δ 1.09) suggested an equatorial position for H-14 within the tetrahydropyran ring of **7** (Figure 2, Supporting Information). Furthermore, 1,3-diaxial NOE correlations were observed between H-13b and Me-26. NOEs were also seen between equatorial Me-25 (δ 1.47) and both H-12 protons (δ 1.72, 2.35). Collectively, these data supported a configuration of 11*R*,14*S* for **7**.

High-resolution mass spectral data of bromophycolide Q (**8**), $[\text{M} - \text{H}]^-$ m/z 581.0869, suggested a molecular formula of $\text{C}_{27}\text{H}_{36}\text{O}_4\text{Br}_2$, as for **4**, **5**, and **7**. The ^1H NMR spectral data for **8** were identical to that of **7**, except for the loss of the exomethylene signals and the presence of one additional methyl group. HMBC correlations from H-5a (δ 3.15) to olefinic carbons C-6 (δ 131.0) and C-19 (δ 132.9), as well as from Me-23 (δ 1.34) to C-6, C-19, and C-20 (δ 32.6), suggested regioisomerization of the double bond in **8** relative to **7**. A configuration of 7*S*,10*R*,11*R*,14*S*,22*S* stereochemistry was proposed for **8** on the basis of similar NOEs observed for **7** and **8** (Supporting Information).

Together, bromophycolides J–Q (**1**–**8**) represent two novel carbon skeletons, two unique tetrahydropyran-containing bromophycolides, plus two regioisomers of previously reported bromophycolide E (**13**) and a regioisomer of bromophycolide A (**9**). Among the 28 known natural products from *C. serratus*, bromophycolide J (**1**) is unique as the only methoxy-substituted metabolite as well as the only bromophycolide bearing a bicyclo[3.1.0]hexane ring in a new carbon skeleton. However, the bicyclo[3.1.0]hexane ring in **1** could have arisen as an artifact from methanolysis of **6**, initiated by cleavage of the C-22–Br bond followed by a ring closure of the bicyclo[3.1.0]hexane by homoallylic substitution of bromine by methanol. Bromophycolides K (**2**) and L (**3**) represent a second novel carbon skeleton, differing from known bromophycolide structural motifs by a proposed biosynthetic 1,2-methyl shift. Both methyl and hydride shifts are common in terpene biosynthesis;⁸ however, **2** and **3** represent the first bromophycolides exhibiting a rearranged

TABLE 2. Antimalarial Activities of Bromophycolides J–Q (**1**–**8**) and Previously Reported Bromophycolides A–I (**9**–**17**) and De bromophycolide A (**18**)

compd	antimalarial IC_{50} (μM)
1	2.7
2	44
3	9.8
4	0.5
5	1.4
6	1.4
7	2.9
8	1.4
9	0.9
10	4.8
11	56
12	0.3
13	0.8
14	18
15	14
16	0.9
17	2.5
18	>100

carbon skeleton. Bromophycolides P (**7**) and Q (**8**) are also structurally distinct from the other natural products of this class, each with a tetrahydropyran ring within the macrocycle that significantly increases the hydrophobicity and conformational rigidity of the molecule. All of these structural features, including stereochemistry, may be accounted for with biosynthetic mechanisms that incorporate the same bromonium intermediate previously suggested for five- and six-membered ring cyclizations in bromophycolides.⁶ The tetrahydropyran ring in **7** and **8** could arise from attack of nucleophilic C-15 hydroxyl on an electrophilic bromonium ion intermediate at C-10–C-11 (Scheme 1a). Another possible biosynthetic route could involve bromohydrin formation at C-10–C-11, as in other bromophycolides, followed by attack of the C-11 hydroxyl onto a C-15 carbocation (Scheme 1b). The structural novelty observed among the diterpene systems within these 28 natural products suggests a high biosynthetic flexibility within this group.

Bromophycolides J–Q (**1**–**8**) exhibited low micromolar activities against the most common and deadly human malaria parasite *Plasmodium falciparum* (malaria tropica), prompting evaluation of antimalarial activities for previously reported bromophycolides A–I (**9**–**17**) and debromophycolide A (**18**, Table 2). Bromophycolides A (**9**), D (**12**), E (**13**), H (**16**), and M (**4**), representing both 15- and 16-membered lactone frameworks, exhibited potent antimalarial activity with IC_{50} 's of 0.3–0.9 μM , suggesting that neither mode of lactonization confers an inherent bioactivity advantage. Furthermore, a macrolide motif appears to be essential for antimalarial activity, considering that nonmacrocyclic callophycoic acids and callophycols also isolated from *C. serratus* were less active against *P. falciparum*.⁷ Current natural product-derived antimalarial drugs include the artemisinines and quinines, of terpene and alkaloid biogenesis, respectively.⁹ Artemisinines are the most active and rapid acting antimalarial agents known today (IC_{50} values <7 nM)^{9,10} and are also cytotoxic to certain types of human cancer cells.¹¹ While multiple treatment options are available, many malaria strains have evolved drug resistance over the past half-century; also, prophylactic drugs remain obscure, thus making the need for new treatments an immediate

(8) Herbert, R. B., Ed. *The Biosynthesis of Secondary Metabolites*, 2nd ed.; Chapman & Hall: London, 1989.

(9) Schlitzer, M. *Arch. Pharm. Chem. Life Sci.* **2008**, *341*, 149–163.

(10) Basco, L. K.; Le Bras, J. *Am. J. Trop. Med. Hyg.* **1993**, *49*, 301–307.

(11) Singh, N. P.; Lai, H. C. *Anticancer Res.* **2004**, *24*, 2277–2280.

SCHEME 1. Possible Biosynthetic Pathways of the Tetrahydropyran Ring Formation in Bromophycolide P (7): (a) Nucleophilic Attack of C-15 Hydroxyl on Bromonium Intermediate at C-10–C-11; (b) Nucleophilic Attack of C-11 Hydroxyl on C-15 Carbocation

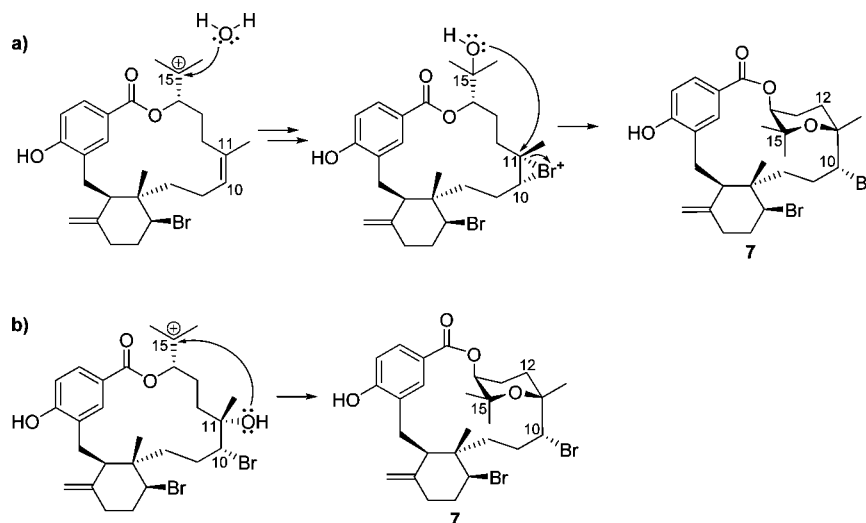


TABLE 3. Pharmacological Activities of Bromophycolides J–Q (1–8)

compd	antibacterial activity (μM)			anticancer activity (μM)			antifungal activity
	MRSA IC ₅₀	VREF IC ₅₀	antitubercular MIC	mean ^a	DU4475 ^b	cell line selectivity (IC ₅₀ max/IC ₅₀ min)	IC ₅₀ (μM) ^c
1	80	66	94	10	3.3	10	NT
2	NT	NT	NT	31	18	3.6	NT
3	8.2	26	49	NT	NT		46
4	6.7	21	>100	3.1	2.1	3.5	>90
5	7.2	56	>50	8.6	1.5	15	44
6	8.9	18	NT	9.7	7.3	3.5	>75
7	1.4	13	48	7.9	21	4.5	45
8	1.8	5.8	22	2.0	2.0	5.5	>90

^a Mean of 12 cancer cell lines (see the Experimental Section for details). ^b breast tumor cell line. ^c Using amphotericin-resistant *Candida albicans*; NT indicates not tested due to insufficient material.

concern.^{9,12} The 15- and 16-membered bromophycolide frameworks represent a new scaffold from which novel and potent antimalarial drugs could be developed.

Of the newly discovered compounds, bromophycolides P (7) and Q (8) exhibited the most potent antibacterial activity against methicillin-resistant *Staphylococcus aureus* (MRSA) and vancomycin-resistant *Enterococcus faecium* (VREF, Table 3), suggesting that the conformational rigidity and/or hydrophobicity conferred by the tetrahydropyran system contributes to antibacterial activity. While all tested bromophycolides exhibited moderate antineoplastic activity, only 5 displayed some cell line selectivity, with an IC₅₀ of 1.5 μM against the breast tumor cell line DU4475, the most sensitive cancer tested (Table 3). Interestingly, while 5 demonstrated cancer cell line selectivity, its regioisomer 4 was quite active against all cancer cell lines tested (IC₅₀'s 2.1–7.2 μM). Bromophycolide Q (8) was the most potent *C. serratus* natural product evaluated (mean anticancer IC₅₀ value of 2.0 μM), but showed little cell line selectivity.

The current study expands the number of bioactive bromophycolide metabolites to 28 and represents two additional novel carbon skeletons, thus suggesting that unexplored red algal families could be an untapped resource of biologically active and interesting natural products.

Experimental Section

Biological Material. *C. serratus* (Harvey ex Kutzing 1957) (family Solieriaceae, order Gigartinales, class Rhodophyceae, phylum Rhodophyta) was collected from Yanuca in the Fiji Islands (18° 23' 57" S, 177° 57' 59" E). Samples were frozen at –20 °C until extraction. Voucher specimens were identified by comparison with previously described morphological traits,¹³ preserved in aqueous formalin, and deposited at the University of the South Pacific in Suva, Fiji, and at Georgia Institute of Technology as ICBG-G-0004, ICBG-G-0005, ICBG-G-0021, and ICBG-G-0049.

Isolation. Frozen *C. serratus* was extracted successively with water, methanol, and methanol/dichloromethane (1:1 and 1:2). Extracts were combined, reduced in vacuo, and subjected to liquid partitioning between methanol/water (9:1) and petroleum ether. The methanol/water ratio of the aqueous fraction was then adjusted to 3:2 and this fraction partitioned against chloroform. The chloroform fraction was subjected to multiple rounds of reversed-phase C₁₈ HPLC (using Agilent Zorbax SB-C₁₈, 5 μm , 9.4 × 250 mm or Alltech Alltima C₁₈, 5 μm , 10 × 250 mm) with a gradient of acetonitrile/water and methanol/water mobile phases, followed by normal-phase silica HPLC (using Agilent RX-SIL columns, 5 μm , 9.4 × 250 mm) with isocratic hexanes/ethyl acetate (82:18) to yield bromophycolides J–Q (1–8). All NMR spectra were collected in CDCl₃ and referenced to residual CHCl₃ (δ 7.24 and 77.0 ppm for ¹H and ¹³C, respectively).

(12) Schiltzer, M. *ChemMedChem* 2007, 2, 944–986.

(13) Littler, D. S.; M. M., L. *South Pacific Reef Plants*; Offshore Graphics, Inc.: Washington, D.C., 2003.

Pharmacological Assays. All pharmacological assays were performed as previously described.^{5–7} Briefly, antimalarial activity was determined with a SYBR Green based parasite proliferation assay, adapted from Smilkstein¹⁴ and Bennett.¹⁵ *P. falciparum* parasites (3D7 strain MR4/ATCC, Manassas, VA) were cultured in human O+ erythrocytes as previously described.¹⁶

Antibacterial assays were performed using methicillin-resistant *S. aureus* (MRSA, ATCC 33591) and vancomycin-resistant *E. faecium* (VREF, ATCC 700221) as test pathogens. Vancomycin and chloramphenicol were used as positive controls for MRSA and VREF, respectively, and DMSO was used as negative control. The optical density was measured at 600 nm using a microplate reader, and the IC₅₀ of each compound was calculated using the dose concentration at 50% inhibition on a sigmoidal dose response curve generated using GraphPad Prism version 4.00 for Windows, GraphPad software, San Diego, CA.

Amphotericin B-resistant *Candida albicans* (ATCC 90873) was used in the antifungal assays. A mixed nystatin/amphotericin B solution was used as a positive control, and DMSO was used as a negative control. The optical density was then measured at 600 nm using a microplate reader, and the IC₅₀ was calculated for each in the same method as the antibacterial assays.

Antitubercular activity was assessed against *Mycobacterium tuberculosis* strain H₃₇Rv (ATCC 27294) using the microplate alamar blue assay (MABA) as described previously.¹⁷ Compounds **1** and **4** were tested at a maximum concentration of 100 μM, and **3**, **5**, **7**, and **8** were tested at a maximum concentration of 50 μM.

Bromophycolides **J** (**1**), **K** (**2**), and **M–Q** (**4–8**) were evaluated against a panel of 12 tumor cell lines including breast, colon, lung, prostate, and ovarian cancer cells. Specific cell lines were as follows: BT-549, DU4475, MDA-MD-468, PC-3, SHP-77, LNCaP-FGC, HCT116, MDA-MB-231, A2780/DDP-S, Du145, CCRF-CEM, and A549. In vitro cytotoxicity was tested with the (3-(4,5-dimethylthiazol-2-yl)-5-(3-carboxymethoxyphenyl)-2-(4-sulfophenyl)-2H-tetrazolium inner salt) MTS dye conversion assay as described previously.¹⁸

Bromophycolide J (1): white amorphous solid (1.0 mg; 0.023% plant dry mass); [α]_D²⁵ +35 (c 0.057 g/100 mL, MeOH); UV (MeOH) λ_{max} (log ε) 265 (3.78) nm; ¹H NMR (CDCl₃, 500 MHz) and ¹³C/DEPT NMR (CDCl₃, 125 MHz) data, Table 1; NOE, COSY, HMBC NMR data, Supporting Information; HRESIMS [M – H][–] m/z 613.1160 (calcd for C₂₈H₃₉O₅Br₂, 613.1164).

Bromophycolide K (2): white amorphous solid (0.8 mg; 0.018% plant dry mass); [α]_D²⁵ +22 (c 0.046 g/100 mL, MeOH); UV (MeOH) λ_{max} (log ε) 264 (3.54) nm; ¹H NMR (CDCl₃, 500 MHz) and ¹³C/DEPT NMR (CDCl₃, 125 MHz) data, Table 1; NOE, COSY, HMBC NMR data, Supporting Information; HRESIMS [M – H][–] m/z 519.1767 (calcd for C₂₇H₃₆O₅Br, 519.1746).

Bromophycolide L (3): white amorphous solid (0.3 mg, 0.007% plant dry mass); [α]_D²⁴ +70 (c 0.033 g/100 mL, MeOH); UV (MeOH) λ_{max} (log ε) 262 (3.72) nm; ¹H NMR (CDCl₃, 500 MHz) and ¹³C NMR (CDCl₃, 125 MHz) data, Table 1; NOE, COSY, and HMBC NMR data, Supporting Information; HRESIMS [M – H][–] m/z 501.1677 (calcd for C₂₇H₃₄O₄Br, 501.1640).

Bromophycolide M (4): white amorphous solid (1.8 mg; 0.041% plant dry mass); [α]_D²³ +68 (c 0.10 g/100 mL, MeOH); UV (MeOH) λ_{max} (log ε) 262 (3.66) nm; ¹H NMR (CDCl₃, 500 MHz) and ¹³C/DEPT NMR (CDCl₃, 125 MHz) data, Table 1; NOE, COSY, HMBC NMR data, Supporting Information; HRESIMS [M – H][–] m/z 581.0906 (calcd for C₂₇H₃₅O₄Br₂, 581.0902).

Bromophycolide N (5): white amorphous solid (1.0 mg, 0.023% plant dry mass); [α]_D²⁴ +101 (c 0.033 g/100 mL, MeOH); UV (MeOH) λ_{max} (log ε) 260 (3.42) nm; ¹H NMR (CDCl₃, 500 MHz) and ¹³C/DEPT NMR (CDCl₃, 125 MHz) data, Table 1; NOE, COSY, and HMBC NMR data, Supporting Information; HRESIMS [M – H][–] m/z 581.0907 (calcd for C₂₇H₃₅O₄Br₂, 581.0902).

Bromophycolide O (6): white amorphous solid (0.5 mg, 0.012% plant dry mass); [α]_D²⁴ +88 (c 0.011 g/100 mL, MeOH); UV (MeOH) λ_{max} (log ε) 260 (3.54) nm; ¹H NMR (CDCl₃, 500 MHz) and ¹³C NMR (CDCl₃, 125 MHz) data, Table 1; NOE, COSY, and HMBC NMR data, Supporting Information; HRESIMS [M – H][–] m/z 661.0182 (calcd for C₂₇H₃₆O₄Br₃, 661.0169).

Bromophycolide P (7): white amorphous solid (4.0 mg, 0.092% plant dry mass); [α]_D²⁴ +120 (c 0.05 g/100 mL, MeOH); UV (MeOH) λ_{max} (log ε) 260 (4.02) nm; ¹H NMR (CDCl₃, 500 MHz) and ¹³C NMR (CDCl₃, 125 MHz) data, Table 1; NOE, COSY, and HMBC NMR data, Supporting Information; HRESIMS [M – H][–] m/z 581.0865 (calcd for C₂₇H₃₅O₄Br₂, 581.0902).

Bromophycolide Q (8): white amorphous solid (1.0 mg, 0.023% plant dry mass); [α]_D²⁴ +102 (c 0.03 g/100 mL, MeOH); UV (MeOH) λ_{max} (log ε) 260 (3.83) nm; ¹H NMR (CDCl₃, 500 MHz) and ¹³C NMR (CDCl₃, 125 MHz) data, Table 1; NOE, COSY, and HMBC NMR data, Supporting Information; HRESIMS [M – H][–] m/z 581.0869 (calcd for C₂₇H₃₅O₄Br₂, 581.0902).

Acknowledgment. This research was supported by the U.S. National Institutes of Health's International Cooperative Biodiversity Groups program (Grant No. U01 TW007401). We thank the Government of Fiji for permission to perform research in their territorial waters and for permission to export samples. We especially thank the Roto Tui Serua and the people of Yanuca Island for facilitating this work. We thank A. Chequer and C. Kicklighter for field assistance; M. Sharma, K. Feussner, and A. Wang for assistance with extractions and separations; B. Smith for insightful experimental comments; T. Davenport and S. Engel for antimicrobial assays; M. C. Sullards and D. Bostwick for mass spectral analyses; L. Gelbaum for NMR assistance; and A. Bommarius and T. Rogers for use of their spectropolarimeter.

Supporting Information Available: 2D NMR data tables (COSY, HMBC, ROESY/NOESY); ¹H, ¹³C, ¹H–¹H COSY, and ROESY NMR spectral data for **1–8**. This material is available free of charge via the Internet at <http://pubs.acs.org>.

JO900008W

(14) Smilkstein, M.; Sriwilajaroen, N.; Kelly, J. X.; Wilairat, P.; Riscoe, M. *Antimicrob. Agents Ch.* **2004**, *48*, 1803–1806.

(15) Bennett, T. N.; Paguio, M.; Gligorijevic, B.; Seudieu, C.; Kosar, A. D.; Davidson, E.; Roepe, P. D. *Antimicrob. Agents Ch.* **2004**, *48*, 1807–1810.

(16) Trager, W.; Jensen, J. B. *Science* **1976**, *193*, 673–675.

(17) Falzari, K.; Zhu, Z.; Pan, D.; Liu, H.; Hongmanee, P.; Franzblau, S. G. *Antimicrob. Agents Ch.* **2005**, *49*, 1447–1454.

(18) Lee, F. Y. F.; Borzilleri, R.; Fairchild, C. R.; Kim, S. H.; Long, B. H.; Reventos-Suarez, C.; Vite, G. D.; Rose, W. C.; Kramer, R. A. *Clin. Cancer Res.* **2001**, *7*, 1429–1437.